Singlet Oxygen Chemistry in Water. 2. Photoexcited Sensitizer Quenching by O_2 at the Water−Porous Glass Interface

Jovan Giaimuccio,[†] Matibur Zamadar,[‡] David Aebisher,[‡] Gerald J. Meyer,[†] and Alexander Greer*,[‡]

Department of Chemistry and Material Science and Engineering, Johns Hopkins University, Baltimore, Maryland 21218, and Department of Chemistry and Graduate Center, City University of New York, Brooklyn College, Brooklyn, New York 11210

Received: August 24, 2008; Revised Manuscript Received: September 26, 2008

Insight into the O_2 quenching mechanism of a photosensitizer (static or dynamic) would be useful for the design of heterogeneous systems to control the mode of generation of $^1O_2$ in water. Here, we describe the use of a photosensitizer, *meso*-tetra(*N*-methyl-4-pyridyl)porphine (**1**), which was adsorbed onto porous Vycor glass (PVG). A maximum loading of 1.1×10^{-6} mol **1** per g PVG was achieved. Less than 1% of the PVG surface was covered with photosensitizer **1**, and the penetration of **1** reaches a depth of 0.32 mm along all faces of the glass. Time-resolved measurements showed that the lifetime of triplet **1*-ads** was 57 μs in water. Triplet O_2 quenched the transient absorption of triplet **1*-ads**; for samples containing 0.9×10^{-6}−0.9×10^{-8} mol **1** adsorbed per g PVG, the Stern−Volmer constant, K_D, ranged from 23 700 to 32 100 M^{-1}. The adduct formation constant, K_S, ranged from 1310 to 510 M^{-1}. The amplitude of the absorption at 470 nm decreased slightly (by about 0.1) with increased O_2 concentrations. Thus, the quenching behavior of triplet **1*-ads** by O_2 was proposed to be strongly dependent on dynamic quenching. Only ∼10% of the quenching was attributed to the static quenching mechanism. The quenching of triplet **1*-ads** was similar to that observed for photosensitizers in homogeneous solution which are often quenched dynamically by O_2.

1. Introduction

Heterogeneous materials have been studied for many years, and chemists discovered that some could be used as supports for the generation of singlet oxygen [$^1O_2(^1\Delta_g)$].[1−1e] Recently, we reported that *meso*-tetra(*N*-methyl-4-pyridyl)porphine (**1**) adsorbed onto porous Vycor glass (PVG), in which a pH decrease of the surrounding solution indicated the displacement of protons from the surface silanol groups via cation exchange (Scheme 1).[2] Singlet oxygen was generated cleanly in aqueous solution upon irradiation of this heterogeneous sensitizer, **1-ads**.[2]

Despite the effectiveness of this and other heterogeneous systems to generate $^1O_2$, surprisingly little is known about the mechanism of sensitizer quenching by O_2 at *water−solid* interfaces. For example, how does the oxygen encounter the excited PVG heterogeneous sensitizer? What mechanism (static or dynamic) converts ground-state O_2 into $^1O_2$, which then diffuses into the bulk solution?

Some detail of the O_2 quenching process may be gleaned from previous studies of *gas−solid* systems. These studies often indicate the static quenching of O_2—where a ground-state O_2 adduct is formed at the surface—rather than a dynamic encounter of O_2 with the surface. At the gas−solid interface, Gafney showed that photoexcited $Ru(bpy)_3^{2+}$-adsorbed to PVG statically quenches O_2,[3] Avnir showed that photoexcited $Ru(bpy)_3^{2+}$-adsorbed to porous silica and porous glass statically quench O_2 at low temperatures, but dynamically quench O_2 at high temperatures,[4] and Thomas showed that aromatic compounds adsorbed onto nonporous glass statically quench O_2.[5,6] Pore size of silica-adsorbed photosensitizers can be tailored to statically or dynamically quench O_2 in gas−solid systems.[7,8]

Few studies have examined sensitizer quenching by O_2 at organic solvent−solid interfaces[9] or water−solid interfaces.[10] Despite reports on $^1O_2$ production (Φ_Δ) and $^1O_2$ lifetimes (τ_Δ) in homogeneous aqueous media, Nafion membranes,[11] micellar media,[12] water-soluble supramolecular hosts,[13] or aqueous reactions using TiO_2,[14] studies of the quenching mechanism of heterogeneous photosensitizers by O_2 at the *water−solid* interface are uncommon and are in need of elaboration.

We report here a photophysical analysis of how O_2 quenches ^{3}**1*** at the water−PVG interface. We also examined the effects of surface loading and percent coverage of the photosensitizer and the depth that **1** can penetrate into the PVG material. An assessment of the quenching of the photosensitizer (static or dynamic) could help in the design of heterogeneous systems that attempt to control the exact mode of generation of $^1O_2$ in water.

2. Experimental Section

2.1. Materials and Sample Preparation. Deionized H_2O was obtained from a U.S. Filter Corp. deionization system. *meso*-Tetra(*N*-methyl-4-pyridyl)porphine tetratosylate was purchased commercially and used as received. The PVG was used as a host material and was purchased from Advanced Glass and Ceramics (Corning 7930). The PVG has a void space of ∼28% of the volume, average pore sizes of 40 Å, a hydrophilic absorbing surface area of 250 m^2/g, a density of 1.38 g/mL, and transparency in the near-UV (50% T at 351 nm), visible, and parts of the near-IR.[15] Pieces of PVG (1.5 cm × 1.5 cm; thickness: 1.15−1.53 mm) were heated in a muffle furnace at 500 °C and stored in a desiccator under vacuum at 30 mmHg.

* Corresponding author. E-mail: agreer@brooklyn.cuny.edu.
† Johns Hopkins University.
‡ City University of New York.

10.1021/jp807556x CCC: $40.75
Published on Web 11/12/2008

SCHEME 1: Adsorption of Photosensitizer 1 onto the PVG Surface and Production of Singlet Oxygen

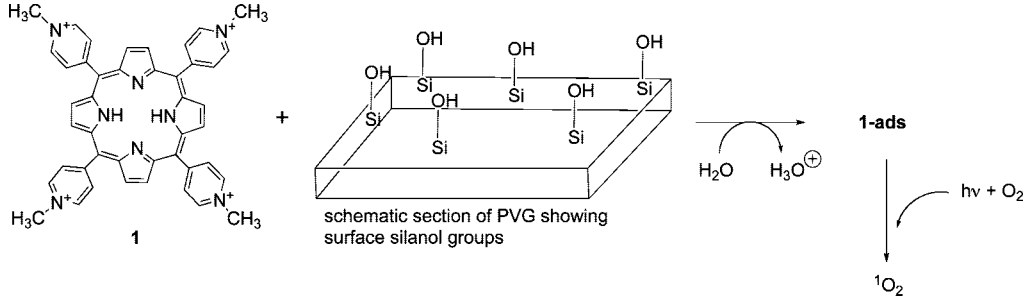

The photosensitizer-coated PVG was prepared by soaking 1.4 g of PVG into a 20 mL 3.7×10^{-5} M aqueous solution of **1** for 15−64 h. The amount of **1** adsorbed onto PVG was calculated from the difference in absorbance of the solution before introduction of PVG and the absorbance of the same solution after the removal of PVG.[2,16] For the transient absorption studies, PVG was cut such that each piece fits diagonally into a 1 cm path-length quartz cuvette. Each PVG/**1** sample was placed into the quartz cuvette, which contained deionized water, and was sparged with N_2 gas for 20 min. Any bubbles that stuck onto the PVG surface were removed by sonication for a few seconds. Some PVG samples (1.5 cm × 1.5 cm; thickness: 1.53 mm) were cut into 0.3 cm × 1.5 cm pieces and photographed with a microscope.

2.2. Instruments. Photographic images were taken with a Nikon TE200 microscope equipped with an Orca 100 monochrome charge-coupled device (CCD) camera and a Hamamatsu camera controller (C4742-95). The light source used was a 100 W mercury arc lamp. The objective used was a Plan Apo 60×Oil DIC. Images were recorded and analyzed with CamMedia software.[17] Absorption spectra were collected with a Hitachi UV−vis U-2001, a Hewlett-Packard 8453 diode array, or a Varian Carey 14 spectrophotometer. In some experiments with the Carey 14 instrument, the Q-bands of **1** at 525, 552, 585, and 640 nm were followed because the intense Soret band at 422 nm gave absorbances of 2.5 or greater, which saturated the UV−vis detector. A Quantel Brilliant B Nd:YAG laser (417 nm, 0.6−1.6 mJ/pulse) was used in the transient absorption experiments.[18,19]

2.3. Transient Absorption Spectroscopy. The PVG samples used in these experiments contained 0.9×10^{-8}−1.1×10^{-6} mol **1**/g PVG. Room-temperature time-resolved measurements were conducted as previously described.[20] The PVG samples were excited at 417 nm but oriented so that reflected laser light was directed at a 45° angle away from the detector on the transient absorption apparatus. Each kinetic trace is an average of 64 laser pulses. The triplet of **1-ads** was monitored at 470 nm, in which a 435 nm long pass filter was placed in front of the detector monochromator to block scattered laser light. The data points in the transient absorption experiments were collected every 10 nm from 450 to 550 nm. An MKS Instruments multigas controller (MKS 647C) was used to control the flow of O_2 and N_2 through two MKS Instruments flow controllers. The flow controllers were set for a flow rate of 100 standard cubic centimeters per minute (sscm). Gas correction factors (GCFs) programmed into the MGC were utilized to correct for specific heat, density, and molecular structure of O_2 and N_2. The samples were purged with different ratios of an O_2:N_2 stream of gas for 5 min before each kinetic trace was taken. The oxygen concentration of a solution bubbled with the O_2:N_2 gas stream were determined by using Henry's law.[21,22]

2.4. Computational Methods. Density function theoretical (DFT) calculations were conducted by the exchange-correlation of B3LYP along with Pople basis set 6-31G(d) with the use of the Gaussian 03 program package.[23] The solvent accessible surface was computed by the method of Lee and Richards.[24]

3. Results and Discussion

3.1. Time-Dependent Adsorption of Photosensitizer onto PVG. A clean piece of PVG placed into an aqueous solution containing **1** led to the adsorption of **1** onto PVG. Figure 1 shows the time-dependent adsorption of **1** onto PVG over a 15 h period. The adsorption process was followed by monitoring the largest of the four Q-bands of **1-ads** at $\lambda = 525$ nm. A plateau is reached when there is 8.8×10^{-7} mol **1** adsorbed onto 1 g PVG. Loadings of 1.1×10^{-6} mol **1** onto PVG can be achieved, but only after a 48−72 h period. Once the **1-ads** samples contained the desired surface coverage, they were rinsed with distilled water prior to use.

3.2. Uniform Photosensitizer Distribution. Absorption spectra were recorded at different points on the PVG film to analyze the dispersal of adsorbed **1**. The Q-band absorptions (475−700 nm) are found to be identical to within 0.01 absorbance unit, suggesting that the distribution of **1** is uniform; thus, the surface coverage of **1** adsorbed onto PVG could then be estimated. Two methods were used to determine the surface coverage of **1** adsorbed onto PVG. Both are in qualitative agreement with each other: (1) The amount of uncoated PVG was determined by subtracting 1.0 g of PVG from (8.83×10^{-7} mol **1**/g PVG × 679.61 g/mol **1**), which is 0.9994 g. Dividing 8.83×10^{-7} mol **1**/g PVG into (0.9994 g uncoated PVG × 250 m^2/g PVG) yielded 3.5×10^{-9} mol **1**/m^2, indicating that

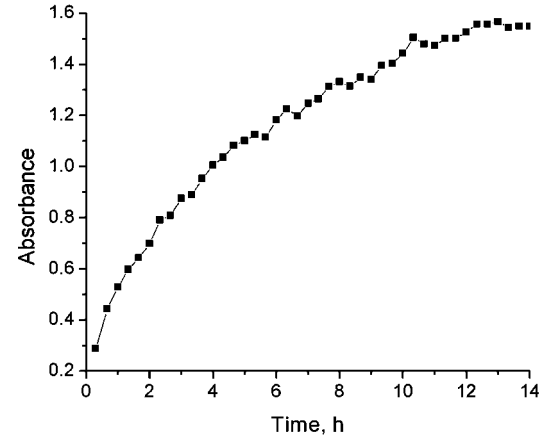

Figure 1. Adsorption of a PVG sample at $\lambda = 525$ nm that was sitting in a solution containing **1**. The PVG sample was removed at the indicated times. The plateau region at 14 h corresponds to 8.83×10^{-7} mol **1** adsorbed onto 1 g PVG.

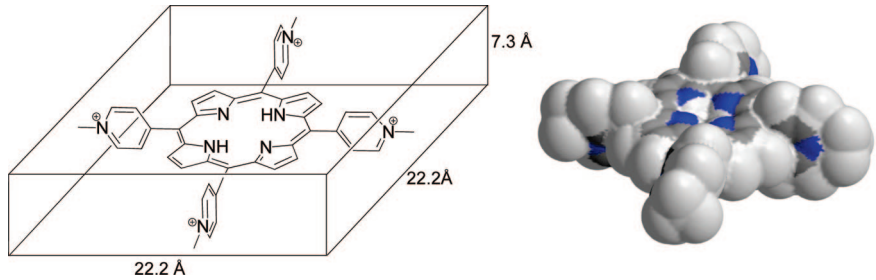

Figure 2. Rectangular shape of **1** (left) estimated from a B3LYP/6-31G(d) optimized structure and the corresponding computed solvent accessible map (right).

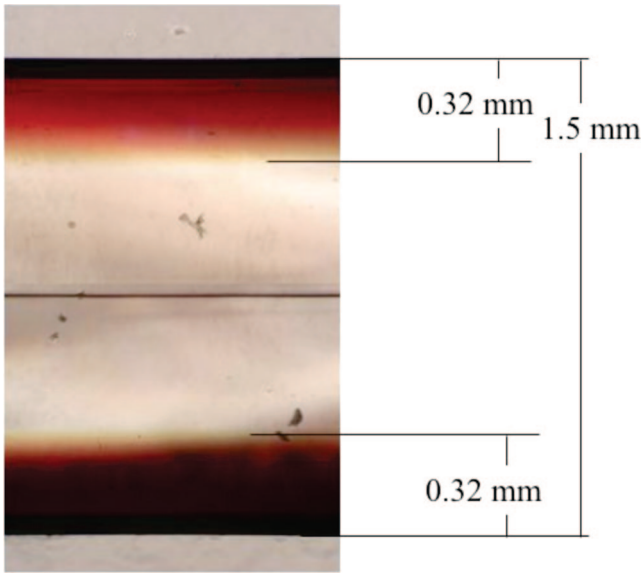

Figure 3. A low-magnification (60×) cross-sectional optical image. The red areas indicate the depth of **1** accessed into PVG. The image shows 0.32 mm penetration depth on each face for 0.9×10^{-6} mol **1** adsorbed onto a 1.5 mm PVG sample. The horizontal line in the middle of the PVG sample corresponds to where two glass layers meet due to the commercial fabrication process.

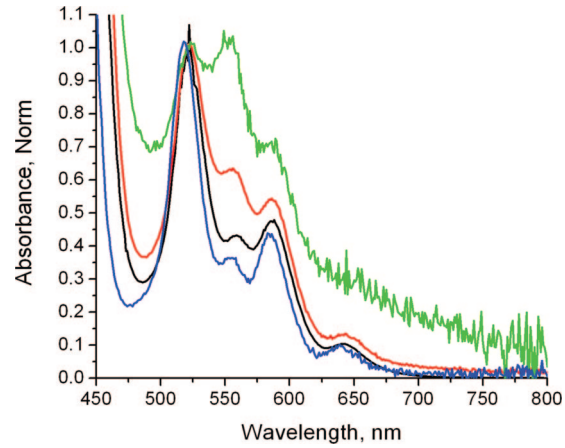

Figure 4. Absorption spectra of **1** in water (blue line) and **1-ads** at different loadings: 0.9×10^{-8} (green line), 0.9×10^{-7} (red line), and 0.9×10^{-6} (black line) mol of **1** adsorbed on PVG. The spectra were normalized at 532 nm. Except for the green line (0.9×10^{-8} mol **1** adsorbed onto PVG), the Q-band maximum is at 525 nm.

0.35% of the PVG surface is covered by **1**. (2) Surface coverage was determined by a calculation, in which porphyrin **1** is taken as a rectangular shape (22.2 Å × 22.2 Å × 7.3 Å) multiplied by (8.83×10^{-7} mol **1**/g PVG × 6.02×10^{23} molecules/mol × 10^{-21} mm^3/Å^3), which equals 1.91 mm^3/g PVG. The rectangular shape of **1** was estimated on the basis of the B3LYP/6-31G(d) optimized structure and the corresponding solvent accessible contour map (Figure 2), in which the pyridinium rings are nearly orthogonal to the plane of the porphyrin (67°). The corresponding weight of **1**-adsorbed PVG (1.91 mm^3 × 1.38 g PVG/mL) equals 2.64 g PVG. Therefore, the surface coverage of **1** onto PVG was calculated by taking [8.83×10^{-7} mol **1**/(2.64 g PVG × 250 m^2/g PVG)] or 1.4×10^{-9} mol **1**/m^2, yielding 0.13% PVG surface coverage by **1**. Both calculations [(1) and (2), vide supra] indicated that <1% of the PVG surface is covered with the photosensitizer **1**. For comparison, the surface coverage of $Ru(bpy)_3^{2+}$ on PVG is <1%,[3] on porous silica is ~6%, and on porous glass is ~10%.[4]

3.3. Photosensitizer Penetration Depth. The depth that **1** can penetrate into PVG was examined using a microscope equipped with a CCD camera. Figure 3 shows a 1.5 mm thick (sensitizer coated) PVG sample, cut so that the depth of **1** penetrated into PVG could be viewed. The microscope image shows the penetration of **1** reaches a maximum depth of 0.32 mm along all faces of the sample, which corresponds to the plateau region of 8.8×10^{-7} mol **1**/g PVG (Figure 1). Although O_2 and other gases are permeable and can pass through the connected pores of PVG,[25] **1** neither penetrates to the center of the PVG film nor is **1** localized on the outer surface of PVG. A 10-fold mole increase of **1** resulted in only a 4-fold local increase in sensitizer distribution into PVG [cf. 0.9×10^{-6} mol **1** (penetration depth 0.32 mm) and 0.9×10^{-7} mol **1** adsorbed onto 1 g PVG (penetration depth 0.09 mm)]. Oxygen is expected to reach the excited sites of **1-ads**, controlled by Knudsen diffusion, in which O_2 collides numerous times within the pore walls, eventually proceeding through the PVG channels. For comparison, $Ru(bpy)_3^{2+}$ penetrates 0.5 ± 0.1 mm into PVG.[3] Streptocyanine dyes also possessed diffusivity into silica gels, influenced by the gel porosities.[26]

3.4. Spectral Properties. Previously, we reported that the spectral features of **1-ads** are nearly identical to **1** in fluid water solution.[2] Here, we report the spectral features measured at different concentrations of **1** adsorbed onto PVG.

Figure 4 shows absorption spectra of **1** in water and **1** adsorbed onto PVG. While the effect of higher coverage dose of **1** produces neither red shifts nor blue shifts in the Q-bands, the adsorption of **1** on PVG leads to an unexpected effect on the absorption intensity. Higher coverages of **1** adsorbed onto PVG led to a *decrease* of the Q-band absorption intensity, (cf. 0.9×10^{-8}, 0.9×10^{-7}, and 0.9×10^{-6} mol **1**/g PVG). At higher surface coverage, the absorption spectrum of **1-ads** becomes somewhat similar to that of **1** in aqueous solution (cf. spectra in blue and black, Figure 4). Deducing a possible orientational effect of the porphyrin on the PVG surface is challenging based upon these normalized absorption spectra. Polarization effects are known for porphyrins result in symmetric changes of all the $S_0 \rightarrow S_1$ transitions. However, atomic-level

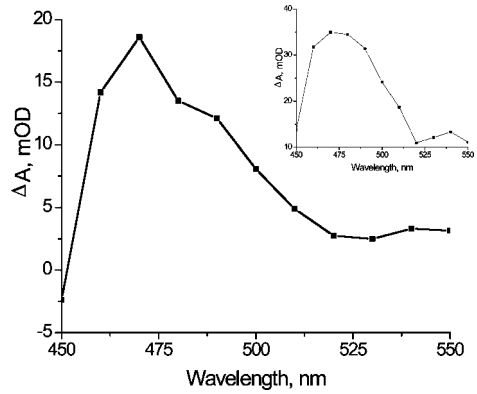

Figure 5. Nanosecond transient absorption spectra observed at 500 ns after pulsed-light excitation (417 nm, 1.6 mJ/pulse) of **1** in water solution (inset) and **1** at the water/PVG interface. Data points were collected every 10 nm from 450 to 550 nm.

detail is unavailable for PVG and how it may relate to the conformation of adsorbed **1**. Interestingly, recent studies have shown a reduced hydrating ability of ~2.2 H-bonds per water molecule confined in PVG pores compared bulk water with ~3.6 H-bonds per water molecule, pointing to the importance for confinement effects.[27,28]

3.5. Time-Resolved Photophysical Studies. Figure 5 shows a nanosecond transient absorption spectrum generated from pulsed 417 nm light excitation of 0.9×10^{-7} mol **1** adsorbed onto 1 g PVG in an N_2-purged H_2O solution. The absorption band at ~470 nm was assigned to **^{3}1*-ads**. Similar transient features were observed for **^{3}1*** in fluid water (Figure 5, inset) and also by Reddi et al. for **^{3}1*** in phosphate buffered solution and in aqueous 2% sodium dodecyl sulfate solution.[29] First-order decay kinetics were observed for the transient absorption of **^{3}1*-ads**, which decayed cleanly to baseline. The lifetime of **^{3}1*-ads** ($\tau_0 = 57 \pm 1$ μs) is similar to **^{3}1*** in fluid aqueous solution ($\tau_0 = 49 \pm 1$ μs). Our absorption measurements in the UV−vis region before and after transient absorption experiments revealed no significant change. Next we describe how O_2 quenches the transient absorption of **^{3}1*-ads** and **^{3}1*** in water solution.

Figure S1 shows the lifetime and the amplitude quenching of the **^{3}1*-ads** transient absorption by O_2 (Supporting Information). Photoexcited **1** quenching by O_2 at the PVG/water interface encouraged a Stern−Volmer analysis for insight into quenching mechanism. Two mechanisms were considered: (1) the dynamic encounter of O_2 with an excited site on the surface, and (2) a ground-state O_2 adduct formed at the surface with migration of adsorbed O_2 to an excited site (Scheme 2).

Stern−Volmer data collected at nine O_2 concentrations (from 0 to 0.4 mM) are shown in Table 1 and Figure 6, in which the symbol τ refers to the lifetime of the excited porphyrin, k_q is the rate constant for O_2 quenching, K_D is the Stern−Volmer constant, K_S is the association constant for complex formation between the sensitizer and O_2, and the subscript "0" indicates data in the absence of O_2. The left axis of Figure 6 shows the plot of τ_0/τ vs $[O_2]$ to be linear over the O_2 concentration examined and corresponded to the Stern−Volmer equation: $\tau_0/\tau = 1 + k_q\tau_0[O_2] = 1 + K_D[O_2]$. For 0.9×10^{-7} mol **1** adsorbed onto 1 g PVG, $K_D = 26\,500$ M^{-1} and the quenching rate constant $k_q = 4.6 \times 10^8$ M^{-1} s^{-1}, indicating that 50% of **^{3}1*-ads** was quenched at an $[O_2]$ of 0.04 mM. For the samples containing 0.9×10^{-6}−0.9×10^{-8} mol **1** adsorbed onto 1 g PVG, the K_D values ranged from 32 000 to 23 700 M^{-1}.

Interestingly, the bimolecular quenching constant k_q for **1-ads** ($k_q = \sim 5 \times 10^8$ M^{-1} s^{-1}) is about one-quarter the value measured for **1** in fluid water ($k_q = 1.8 \times 10^9$ M^{-1} s^{-1}). The experiments for **1** in fluid water solution produced a K_D value of 89 600 M^{-1}. Thus, the time scale for O_2 diffusion may be slower in the water−PVG heterogeneous system compared to fluid solution. By analogy, Thomas et al. used the Einstein equation $\langle x^2 \rangle = 6Dt$ to suggest that nitromethane quenching of excited anthracene is 10^3−10^6 times slower in a zeolite compared to fluid solution (cf. 10^{-8}−10^{-11} cm^2 s^{-1}).[30] In our system, the smaller K_D values in the heterogeneous samples may result from reduced directions for access of O_2 to **^{3}1*-ads** compared to O_2 to **^{3}1*** in fluid solution.

The amplitude of the time-resolved absorbance at 470 nm was examined (Figure S1, Supporting Information). Because a

SCHEME 2: Mechanism of ^{3}1*-ads Quenching by O_2[a]

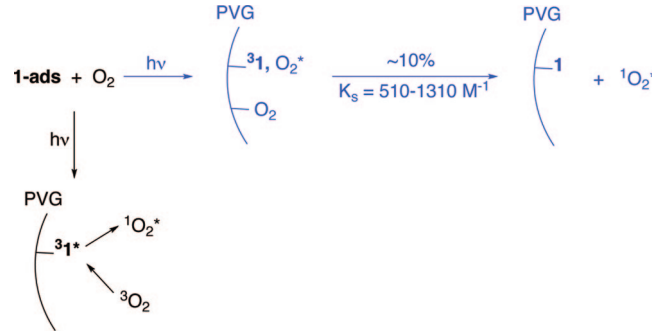

[a] Dynamic quenching route in black and static quenching route in blue.

TABLE 1: Stern−Volmer Quenching Constants as a Function of Coverage of 1 onto Porous Vycor Glass or of 1 in Fluid Water Solution

photosens	absorbance λ_{520}	K_D (M^{-1})	K_S (M^{-1})	k_q (M^{-1} s^{-1})
1-ads[a,b]	0.87	23700 ± 1320	1310 ± 210	4.2×10^8
1-ads[a,c]	0.25	26500 ± 1220	510 ± 60	4.6×10^8
1-ads[a,d]	0.025	32100 ± 1460	650 ± 80	5.6×10^8
1 in fluid H_2O[e]	~0.2	89600 ± 2600	1160 ± 170	1.8×10^9

[a] The PVG/**1** samples were immersed in water. [b] Sample contained 0.9×10^{-6} mol **1** adsorbed onto PVG. [c] Sample contained 0.9×10^{-7} mol **1** adsorbed onto PVG. [d] Sample contained 0.9×10^{-8} mol **1** adsorbed onto PVG. [e] Homogeneous **1** in deionized water solution.

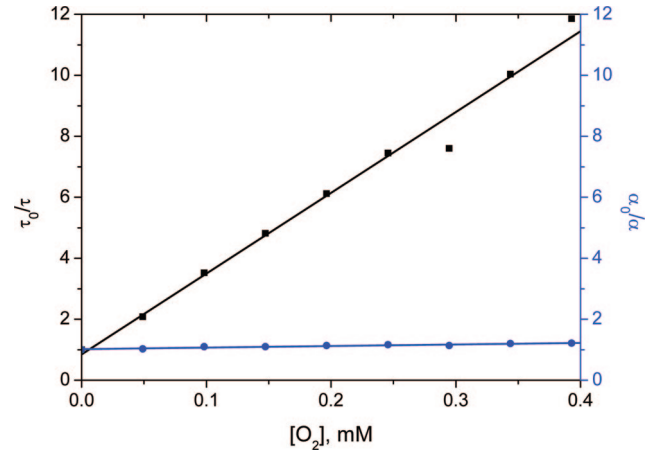

Figure 6. Lifetime quenching as a function of O_2 concentration of a H_2O solution containing 0.9×10^{-7} mol **1** adsorbed onto PVG (in black, left). Amplitude quenching as a function of O_2 concentration of a H_2O solution containing 0.9×10^{-7} mol **1** adsorbed onto PVG (in blue, right). Samples were excited with a 10 ns 417 nm light pulse (0.6 mJ/pulse), and the transient absorption was monitored at 470 nm.

ground-state adduct equilibrium of **1-ads** and O_2 would be expected to have a different absorption spectrum from **1-ads**, an absorption decrease can point to a static quenching mechanism. Figure 6 (right-hand *Y*-axis) shows the plot of α_0/α vs $[O_2]$ was linear over the O_2 concentration examined and followed the equation $\alpha_0/\alpha = 1 + K_S[O_2]$. For **1-ads**, the adduct formation constant K_S ranged from 510 to 1310 M^{-1}. The amplitude of the absorption at 470 nm decreased slightly (by about 0.1) with increasing O_2 concentrations. Thus, we estimate that ~10% of the quenching occurred via the static quenching mechanism (colored blue in Scheme 2). The above Stern−Volmer analysis suggested that quenching of ^{3}**1*-ads** by O_2 is primarily dynamic, the route colored black in Scheme 2. In the absence of aggregation, photosensitizers in homogeneous fluid solution are often quenched dynamically by O_2.[21]

4. Conclusion

In isotropic heterogeneous media static and dynamic quenching modes can operate. In the present case, we have evidence that O_2 quenches triplet **1*** at the water−PVG interface primarily by a dynamic quenching mechanism. The contribution from static quenching remains low even with loadings of **1** onto PVG that varied by 100-fold. The O_2 quenching constants k_q for ^{3}**1*-ads** were only 3−4 times smaller than for ^{3}**1*** itself, suggesting the heterogeneous system is capable of generating singlet oxygen for its use as a reagent in the surrounding aqueous solution.

Acknowledgment. J.G. and G.J.M. thank the National Science Foundation for support. D.A., M.Z., and A.G. thank the National Institutes of Health and the PSC-CUNY Grants Program for support. Computational support was provided by the CUNY Graduate Center computational facility. We thank Harry D. Gafney (CUNY Queens College) for valuable discussions in an early phase of this study.

Supporting Information Available: Time-resolved absorbance of ^{3}**1*-ads** in the presence of increasing concentrations of oxygen. This material is available free of charge via the Internet at http://pubs.acs.org.

References and Notes

(1) Recent examples include: (a) Polymers and polymer blends: Koizumi, H.; Kimata, Y.; Shiraishi, Y.; Hirai, T. *Chem. Commun.* **2007**, 1846–1848. Schaap, A. P. *Spectrum* **2007**, *20*, 4–13. Zebger, I.; Poulsen, L.; Gao, Z.; Andersen, L. K.; Ogilby, P. R. *Langmuir* **2003**, *19*, 8923–8933. (b) Quantum dots: Ma, J.; Chen, J.-Y.; Idowu, M.; Nyokong, T. *J. Phys. Chem. B* **2008**, *112*, 4465–4469. Tsay, J. M.; Trzoss, M.; Shi, L.; Kong, X.; Selke, M.; Jung, M. E.; Weiss, S. *J. Am. Chem. Soc.* **2007**, *129*, 6865–6871. Samia, A. C. S.; Dayal, S.; Burda, C. *Photochem. Photobiol.* **2006**, *82*, 617–25. (c) Silica, silica nanoparticles, xerogels, and exchange resins: Cantau, C.; Pigot, T.; Manoj, N.; Oliveros, E.; Lacombe, S. *ChemPhysChem* **2007**, *8*, 2344–2353. Feng, K.; Wu, L.-Z.; Zhang, L.-P.; Tung, C.-H. *Tetrahedron* **2007**, *63*, 4907–4911. Ishii, K.; Shiine, M.; Kikukawa, Y.; Kobayashi, N.; Shiragami, T.; Matsumoto, J.; Yasuda, M.; Suzuki, H.; Yokoi, H. *Chem. Phys. Lett.* **2007**, *448*, 264–267. Chirvony, V.; Chyrvonaya, A.; Ovejero, J.; Matveeva, E.; Goller, B.; Kovalev, D.; Huygens, A.; de Witte, P. *Adv. Mater.* **2007**, *19*, 2967–2972. Greer, A. *Acc. Chem. Res.* **2006**, *39*, 797–804. Roy, I.; Ohulchanskyy, T. Y.; Pudavar, H. E.; Bergey, E. J.; Oseroff, A. R.; Morgan, J.; Dougherty, T. J.; Prasad, P. N. *J. Am. Chem. Soc.* **2003**, *125*, 7860–7865. (d) Modified TiO_2: Naito, K.; Tachikawa, T.; Fujitsuka, M.; Majima, T. *J. Phys. Chem. C* **2008**, *112*, 1048–1059. Jaczyk, A.; Krakowska, E.; Stochel, G.; Macyk, W. *J. Am. Chem. Soc.* **2006**, *128*, 15574–15575. Tatsuma, T.; Tachibana, S.; Miwa, T.; Tryk, D. A.; Fujishima, A. *J. Phys. Chem. B* **1999**, *103*, 8033–8035. (e) Zeolites: Cojocaru, B.; Laferriere, M.; Carbonell, E.; Parvulescu, V.; Garcia, H.; Scaiano, J. C. *Langmuir* **2008**, *24*, 4478–4481. Pace, A.; Pierro, P.; Buscemi, S.; Vivona, N.; Clennan, E. L. *J. Org. Chem.* **2007**, *72*, 2644–2646. Jockusch, S.; Sivaguru, J.; Turro, N. J.; Ramamurthy, V. *Photochem. Photobiol. Sci.* **2005**, *4*, 403–405.

(2) Aebisher, D.; Azar, N. S.; Zamadar, M.; Gafney, H. D.; Gandra, N.; Gao, R.; Greer, A. *J. Phys. Chem. B* **2008**, *112*, 1913–1917.

(3) Gafney, H. D.; Wolfgang, S. *J. Phys. Chem.* **1983**, *87*, 5395–5401.

(4) Samuel, J.; Ottolenghi, M.; Avnir, D. *J. Phys. Chem.* **1992**, *96*, 6398–6405.

(5) Krasnansky, R.; Koike, K.; Thomas, J. K. *J. Phys. Chem.* **1990**, *94*, 4521.

(6) Krasnansky, R.; Thomas, J. K. *J. Photochem. Photobiol. A: Chem.* **1991**, *57*, 81–86.

(7) Drake, J. M.; Levitz, P.; Turro, N. J.; Nitsche, K. S.; Cassidy, K. F. *J. Phys. Chem.* **1988**, *92*, 4680–4684.

(8) Wellner, E.; Rojanski, D.; Ottolenghi, M.; Huppert, D.; Avnir, D. *J. Am. Chem. Soc.* **1987**, *109*, 575–576.

(9) Ruetten, S. A.; Thomas, J. K. *J. Phys. Chem. B* **1999**, *103*, 1278–1286.

(10) Xiong, Z.; Xu, Y.; Zhu, L.; Zhao, J. *Environ. Sci. Technol.* **2005**, *39*, 651–657.

(11) (a) Zhang, D.; Wu, L.-Z.; Yang, Q.-Z.; Li, X.-H.; Zhang, L.-P.; Tung, C.-H. *Org. Lett.* **2003**, *5*, 3221–3224. (b) Wetzler, D. E.; Garcia-Fresnadillo, D.; Orellana, G. *Phys. Chem. Chem. Phys.* **2006**, *8*, 2249–2256.

(12) (a) Rodgers, M. A. J.; Lee, P. C. *J. Phys. Chem.* **1984**, *88*, 3480–3484. (b) Lee, P. C.; Rodgers, M. A. J. *J. Phys. Chem.* **1984**, *88*, 4385–4389. (c) Matheson, I. B. C.; Rodgers, M. A. J. *J. Phys. Chem.* **1982**, *86*, 884–887. (d) Lee, P. C.; Rodgers, M. A. J. *J. Phys. Chem.* **1983**, *87*, 4894–4898.

(13) Natarajan, A.; Kaanumalle, L. S.; Jockusch, S.; Gibb, C. L. D.; Gibb, B. C.; Turro, N. J.; Ramamurthy, V. *J. Am. Chem. Soc.* **2007**, *129*, 4132–4133.

(14) Daimon, T.; Nosaka, Y. *J. Phys. Chem. C* **2007**, *111*, 4420–4424.

(15) Elmer, T. H. In *ASM Engineered Materials Handbook*; Schnieder, S. J., Jr. , Ed.; ASM: Materials Park, OH, 1991; Vol. 4, p 427.

(16) Gafney, H. D.; Shi, W. *J. Phys. Chem.* **1988**, *92*, 2329.

(17) Bauer, L. A.; Reich, D. H.; Meyer, G. J. *Langmuir* **2003**, *19*, 7043–7048.

(18) Staniszewski, A.; Morris, A. J.; Ito, T.; Meyer, G. J. *J. Phys. Chem. B* **2007**, *111*, 6822–6828.

(19) Staniszewski, A.; Heuer, W. B.; Meyer, G. J. *Inorg. Chem.* **2008**, *47*, 7062–7064.

(20) Argazzi, R.; Bignozzi, C. A.; Heimer, T. A.; Castellano, F. N.; Meyer, G. J. *Inorg. Chem.* **1994**, *33*, 5741–5749.

(21) Iu, K.-K.; Ogilby, P. R. *J. Phys. Chem.* **1988**, *92*, 4662–4666.

(22) Battino, R., Ed. *IUPAC Solubility Data Series*; Pergamon: Oxford, 1981; Vol. 7.

(23) Frisch, M. J.; Trucks, G. W.; Schlegel, H. B.; Scuseria, G. E.; Robb, M. A.; Cheeseman, J. R.; Montgomery, J. A., Jr.; Vreven, T.; Kudin, K. N.; Burant, J. C.; Millam, J. M.; Iyengar, S. S.; Tomasi, J.; Barone, V.; Mennucci, B.; Cossi, M.; Scalmani, G.; Rega, N.; Petersson, G. A.; Nakatsuji, H.; Hada, M.; Ehara, M.; Toyota, K.; Fukuda, R.; Hasegawa, J.; Ishida, M.; Nakajima, T.; Honda, Y.; Kitao, O.; Nakai, H.; Klene, M.; Li, X.; Knox, J. E.; Hratchian, H. P.; Cross, J. B.; Bakken, V.; Adamo, C.; Jaramillo, J.; Gomperts, R.; Stratmann, R. E.; Yazyev, O.; Austin, A. J.; Cammi, R.; Pomelli, C.; Ochterski, J. W.; Ayala, P. Y.; Morokuma, K.; Voth, G. A.; Salvador, P.; Dannenberg, J. J.; Zakrzewski, V. G.; Dapprich, S.; Daniels, A. D.; Strain, M. C.; Farkas, O.; Malick, D. K.; Rabuck, A. D.; Raghavachari, K.; Foresman, J. B.; Ortiz, J. V.; Cui, Q.; Baboul, A. G.; Clifford, S.; Cioslowski, J.; Stefanov, B. B.; Liu, G.; Liashenko, A.; Piskorz, P.; Komaromi, I.; Martin, R. L.; Fox, D. J.; Keith, T.; Al-Laham, M. A.; Peng, C. Y.; Nanayakkara, A.; Challacombe, M.; Gill, P. M. W.; Johnson, B.; Chen, W.; Wong, M. W.; Gonzalez, C.; Pople, J. A. Gaussian 03, revision B.05; Gaussian, Inc., Pittsburgh, PA, 2003.

(24) (a) Lee, B.; Richards, F. M. *J. Mol. Biol.* **1971**, *55*, 379–380. (b) Richards, F. M. *Annu. Rev. Biophys. Bioeng.* **1977**, *6*, 151–176.

(25) (a) Knagge, K.; Smith, J. R.; Smith, L. J.; Buriak, J.; Raftery, D. *Solid State Nucl. Magn. Reson.* **2006**, *29*, 85–89. (b) Preethi, N.; Shinohara, H.; Nishide, H. *Bull. Chem. Soc. Jpn.* **2006**, *79*, 1308–1311. (c) Uchytil, P.; Petrickovic, R.; Seidel-Morgenstern, A. *J. Membr. Sci.* **2007**, *293*, 15–21. (d) Shiojiri, K.; Yanagisawa, Y.; Yamasaki, A.; Kiyono, F. *J. Membr. Sci.* **2006**, *282*, 442–449. (e) Yang, J.; Cermakova, J.; Uchytil, P.; Hamel, C.; Seidel-Morgenstern, A. *Catal. Today* **2005**, *104*, 344–351.

(26) Hellriegel, C.; Kirstein, J.; Braeuchle, C.; Latour, V.; Pigot, T.; Olivier, R.; Lacombe, S.; Brown, R.; Guieu, V.; Payrastre, C.; Izquierdo, A.; Mocho, P. *J. Phys. Chem. B* **2004**, *108*, 14699–14709.

(27) Gleb, L. D.; Gubbins, K. E. *Langmuir* **1998**, *14*, 2097–2111.

(28) Thompson, H.; Soper, A. K.; Ricci, M. A.; Bruni, F.; Skipper, N. T. *J. Phys. Chem. B* **2007**, *111*, 5610–5620.

(29) Reddi, E.; Ceccon, M.; Valduga, G.; Jori, G.; Bommer, J. C.; Elisei, F.; Latterini, L.; Mazzucato, U. *Photochem. Photobiol.* **2002**, *75*, 462–470.

(30) Ellison, E. H.; Thomas, J. K. *Langmuir* **2001**, *17*, 2446–2454.

JP807556X